ISSN 2616-5880 Vol. 7, Issue 1: 80-88, DOI: 10.25236/AJMC.2026.070112

Preparation and Sustained-Release Properties of Panax notoginseng Leaf Saponins-Loaded Multi-Walled Carbon Nanotubes/Chitosan Composite Gel

Fu-neng Tan*

Wenshan University, Wenshan, 663099, Yunnan, China

Abstract: *To address the intrinsic drawbacks of pure drug-loaded chitosan hydrogels—namely poor mechanical strength, severe initial burst release, and insufficient structural stability—this work developed a multi-walled carbon nanotube (MWCNT)/chitosan composite hydrogel loaded with Panax notoginseng leaf saponins (LPNS). Systematic characterization of its microstructure, stability, and sustained-release performance was conducted to provide experimental support for developing local delivery carriers for active ingredients of traditional Chinese medicine. The composite hydrogel was fabricated via ultrasonic dispersion coupled with physical crosslinking. MWCNT loading was optimized using visual appearance, swelling ratio, and mechanical properties as evaluation criteria, while LPNS loading was optimized based on encapsulation efficiency and drug loading capacity. Intermolecular interactions among components were analyzed via Fourier transform infrared spectroscopy (FT-IR). Swelling kinetics, thermal stability, and in vitro drug release profiles were investigated, and the release mechanism was elucidated through kinetic modeling. At optimal loadings of 0.045 g MWCNTs and 0.07 g LPNS, the resultant composite hydrogel was homogeneously dispersed, yielding a 37.2% improvement in tensile strength relative to pure chitosan hydrogel, alongside an encapsulation efficiency of 97.47% and drug loading capacity of 3.34%. It reached a swelling ratio of 491% after 4 h of immersion in pH 7.4 PBS, and retained structural integrity after 24 h of storage at both 4 °C and 60 °C, demonstrating markedly superior stability to the pure chitosan counterpart. The in vitro release profile featured a suppressed initial burst and prolonged sustained release, with 68.3% cumulative drug release at 48 h. The release kinetics best fitted the Higuchi model (R^2 = 0.9912), with a Fickian diffusion-dominated release mechanism. Collectively, the incorporation of MWCNTs effectively reinforces the mechanical strength and structural stability of chitosan hydrogels and significantly retards LPNS release. This composite hydrogel holds great promise for local sustained delivery of traditional Chinese medicine active ingredients.*

Keywords: *Panax notoginseng leaf saponins, multi-walled carbon nanotubes , chitosan; composite gel, drug sustained release, kinetic fitting*

1. Introduction

Chitosan (CS) is a naturally abundant alkaline polysaccharide extensively employed as a matrix for drug delivery carriers, owing to its favorable biocompatibility, biodegradability, and film-/gel-forming capabilities [1]. Nevertheless, pure chitosan hydrogels suffer from intrinsic limitations, including low mechanical strength, susceptibility to structural collapse upon swelling, and limited loading capacity for water-soluble drugs, rendering them unable to meet the demands of long-term sustained drug delivery [2]. Accordingly, enhancing the comprehensive performance of chitosan hydrogels via composite modification with inorganic nanomaterials has become a growing focus in biomedical materials research.

Multi-walled carbon nanotubes (MWCNTs) possess an ultrahigh specific surface area, outstanding mechanical properties, and modifiable surface functional groups. As a rigid reinforcing phase embedded in polymer matrices, they concurrently enhance the mechanical strength and interfacial adsorption capacity of composite materials [3]. Accumulating evidence demonstrates that when compounded with chitosan, MWCNTs form a denser three-dimensional network via hydrogen bonding and electrostatic interactions, which not only improves the mechanical performance of hydrogels but also extends the diffusion pathlength of drug molecules and strengthens the sustained-release effect [4]. However, most prior studies have focused on the loading of chemically synthesized drugs. Research into the drug loading mechanisms and release behaviors of MWCNT/chitosan composite hydrogels for saponin active ingredients from traditional Chinese medicine remains limited, and systematic assessments of structural

ISSN 2616-5880 Vol. 7, Issue 1: 80-88, DOI: 10.25236/AJMC.2026.070112

stability are scarce.

Panax notoginseng leaf saponins (LPNS) are dammarane-type tetracyclic triterpenoids extracted from the stems and leaves of Panax notoginseng. They exert multiple pharmacological effects, including anti-inflammatory, analgesic, and microcirculation-improving activities, and hold considerable promise for cutaneous wound repair and local anti-inflammatory therapy [5]. Nonetheless, LPNS exhibit high water solubility, and conventional hydrogel carriers are prone to pronounced initial burst release and a short duration of action, restricting their utility in local administration.

To address this research gap, LPNS were selected as the model active compound, and MWCNTs were employed as both the reinforcing and adsorptive phase to fabricate LPNS-loaded MWCNT/chitosan composite hydrogels via a physical crosslinking strategy. The formulation was optimized through single-factor experiments, and intermolecular interactions among components were characterized via infrared spectroscopy. The swelling kinetics, thermal stability, and in vitro drug release behavior of the hydrogels were systematically investigated, and the release mechanism was elucidated via kinetic model fitting. This work provides an experimental foundation and theoretical reference for developing novel sustained-release formulations of Panax notoginseng leaf saponins.2 Experimental

2 Reagents and Instruments

2.1 Reagents

Chitosan (deacetylation degree ≥ 90%, biochemical grade; Xi'an Tianmao Baoding Biotechnology Co., Ltd., Xi'an, China); multi-walled carbon nanotubes (outer diameter: 10–20 nm, length: 10–30 μm, purity ≥ 95%, high-purity research grade; Shenzhen Turing Evolution Technology Co., Ltd., Shenzhen, China); Panax notoginseng leaf saponins (total saponin content ≥ 80%, food grade; Xi'an Xinlu Biotechnology Co., Ltd., Xi'an, China). Glacial acetic acid, sodium hydroxide, disodium hydrogen phosphate, potassium dihydrogen phosphate, sodium chloride, and potassium chloride were all of analytical grade (Sichuan Xilong Science Co., Ltd., Chengdu, China). Potassium bromide (spectral pure) was purchased from Tianjin Guangfu Fine Chemical Research Institute (Tianjin, China). Distilled water was used for all experiments.

2.2 Instruments

An IRPrestige-21 Fourier transform infrared spectrometer (Shimadzu Corporation, Kyoto, Japan), a Specord 200 UV-Vis spectrophotometer (Analytik Jena AG, Jena, Germany), a 101 electric blast drying oven (Beijing Yongguang Medical Instrument Factory, Beijing, China), a PL203 electronic analytical balance (Ohaus Instruments Co., Ltd., Parsippany, NJ, USA), a 78-1 magnetic heating stirrer (Changzhou Jintan Dadi Automation Instrument Factory, Changzhou, China), an HH-S2s digital constant-temperature water bath (Jintan Dadi Automation Instrument Factory), an SK series ultrasonic cleaner (Shanghai Kedao Ultrasonic Instrument Co., Ltd., Shanghai, China), a THZ-82A desktop constant-temperature oscillation incubator (Changzhou Guohua Electric Appliance Co., Ltd.), a PHS-3C precision pH meter (Shanghai Hongyi Instrument Co., Ltd.), and a WDW-10 universal electronic testing machine (Jinan Shidai Shijin Testing Machine Co., Ltd., Jinan, China) were used in this study.

2.3 Preparation of Composite Gels

2.3.1 Preparation of Pure Chitosan Gel

1% (v/v) acetic acid solution was prepared. 1.0 g of chitosan was slowly added to 30 mL of acetic acid solution, stirred magnetically at 40 ℃ until completely dissolved, defoamed at rest, poured into a petri dish, and left to form at room temperature. The obtained pure chitosan gel was denoted as CS group.

2.3.2 Preparation and Optimization of MWCNTs/Chitosan Composite Gels

0.015, 0.030, 0.045, 0.060, and 0.075 g of MWCNTs were respectively added to 30 mL of 1% chitosan acetic acid solution, dispersed ultrasonically for 30 min (power 200 W), stirred magnetically at 40 ℃ evenly, poured into petri dishes, and left to form at room temperature. Composite gels with different MWCNTs contents were obtained and denoted as M1–M5 groups. The optimal addition amount of MWCNTs was determined with appearance, swelling ratio, and tensile strength as evaluation indicators.

ISSN 2616-5880 Vol. 7, Issue 1: 80-88, DOI: 10.25236/AJMC.2026.070112

2.3.3 Preparation of Drug-Loaded Composite Gels

0.05, 0.06, 0.07, 0.08, and 0.09 g of LPNS were respectively added to the MWCNTs/chitosan mixture with the optimal ratio, stirred at 40 ℃ until completely dissolved, defoamed by ultrasound, poured into petri dishes, and left to form at room temperature. LPNS-MWCNTs/chitosan composite gels with different drug loadings were obtained and denoted as D1–D5 groups. Meanwhile, pure chitosan drug-loaded gel without MWCNTs was prepared as the control group.

2.4 Performance Tests and Characterization

2.4.1 Evaluation of Appearance and Dispersibility

The surface morphology, uniformity, and transparency of each group of gels were observed at room temperature, and the agglomeration was recorded for qualitative evaluation.

2.4.2 Swelling Property Test

Gel samples were cut into small pieces of 1 cm × 1 cm × 0.5 cm, dried at 100 ℃ to constant weight, and the dry weight W_0 was recorded. The dry gels were immersed in pH 7.4 PBS buffer and kept at 37 ℃. Samples were taken out at 1, 2, 3, and 4 h respectively, and the wet weight W_n was recorded after absorbing the surface free water with filter paper. The swelling ratio (SR) was calculated according to Equation (1). Each group was measured in parallel for 3 times.

$$SR=\frac{W_n-W_0}{W_0}\times 100\% \quad (1)$$

2.4.3 Mechanical Property Test

The gels were made into long strip specimens of 80 mm×10 mm×2 mm. The tensile properties were tested by a universal electronic testing machine, with a tensile rate of 10 mm/min and a fixture spacing of 50 mm. The tensile strength and elongation at break were determined. Three specimens were tested in parallel for each group, and the average value was taken.

2.4.4 Drug-Loading Performance Determination

The content of LPNS was determined by ultraviolet spectrophotometry. A series of standard PBS solutions of *Panax notoginseng* leaf saponins with concentrations of 0.01–0.05 mg/mL were precisely prepared. The maximum absorption wavelength was determined to be 250 nm by full-wavelength scanning. The absorbance was measured and the standard curve was drawn, with the regression equation A=77.48C+0.023 (R^2=0.9992) and good linear relationship.

The drug-loaded gel was centrifuged at high speed (4 000 r/min, 15 min). The supernatant was diluted and the absorbance at 250 nm was measured to calculate the mass of free drug. The encapsulation efficiency (EE) and drug loading capacity (DLC) were calculated according to Equation (2) and (3). Each group was measured in parallel for 3 times.

$$EE=\frac{m_{total}-m_{free}}{m_{total}}\times 100\% \quad (2)$$

$$DLC=\frac{m_{total}-m_{free}}{m_{dry\ mass\ of\ xerogel}}\times 100\% \quad (3)$$

m_{total} is the total mass of added LPNS, g; m_{free} is the mass of free saponins in the supernatant, g.

2.4.5 Cold and Heat Resistance Test

Two equal gel samples were placed in a refrigerator at 4 ℃ and a constant temperature drying oven at 60 ℃ respectively. After being stored for 12 h and 24 h, the samples were taken out to observe the changes in appearance and morphology, and the mass retention rate was measured to evaluate the temperature stability.

2.4.6 FT-IR Characterization

The dry gel was ground into fine powder, mixed and ground with potassium bromide at a mass ratio of 1:100, and pressed into tablets for infrared scanning. The scanning range was 4 000–400 cm^{-1}, the resolution was 4 cm^{-1}, and the scanning times were 32.

2.4.7 In Vitro Release Experiment

The *in vitro* drug release behavior was determined by dialysis bag method (molecular weight cut-off

ISSN 2616-5880 Vol. 7, Issue 1: 80-88, DOI: 10.25236/AJMC.2026.070112

8 000–14000 Da). 1.5 g of drug-loaded gel was weighed into a dialysis bag, 5 mL of pH 7.4 PBS buffer was added, both ends were sealed after exhausting air bubbles, and then the bag was placed in a conical flask containing 200 mL of PBS buffer. The flask was placed in a constant temperature oscillation incubator (37 ℃, 150 r/min). 2 mL of sample was taken at 0.5, 1, 2, 4, 8, 12, 24, 36, and 48 h respectively, and an equal volume of fresh isothermal PBS buffer was supplemented at the same time.After filtration through a 0.45 μm membrane, the absorbance of the sample at 250 nm was measured, the cumulative release rate was calculated, and the release curve was plotted. Four common models, including zero-order kinetics, first-order kinetics, Higuchi, and Ritger-Peppas, were used to fit the release data, and the release mechanism was judged according to the correlation coefficient R^2.

2.5 Statistical Analysis

All experiments were repeated for 3 times. The data were statistically analyzed by SPSS 22.0 software. One-way analysis of variance was used for comparison between groups, and $P<0.05$ was considered statistically significant.

3. Results and Discussion

3.1 Effect of MWCNTs Dosage on Composite Gel Properties

3.1.1 Appearance and Dispersibility

The appearance characteristics of gels with different MWCNTs dosages are shown in Table 1. When the addition amount of MWCNTs was ≤ 0.045 g, the gel surface was smooth and delicate without visible agglomerated particles, presenting a uniform gray-black translucent state. When the addition amount exceeded 0.060 g, granular agglomerates appeared on the gel surface, and the transparency decreased significantly. This is because at low dosage, MWCNTs can be uniformly dispersed in chitosan solution by ultrasound, forming good interfacial bonding with polymer chains; at excessive dosage, the van der Waals force and π-π stacking interaction between carbon nanotubes are enhanced, which easily causes winding and agglomeration and destroys the homogeneity of the gel [6].

Table 1 Appearance and dispersibility of gels with different MWCNTs dosages

Group	MWCNTs dosage / g	appearance morphology	dispersibility evaluation
CS	0	colorless and transparent, smooth surface	—
M1	0.015	light gray and translucent, smooth surface	good, no agglomeration
M2	0.030	gray and translucent, uniform surface	good, no obvious agglomeration
M3	0.045	dark gray and translucent, uniform texture	excellent, no agglomeration
M4	0.060	gray-black and opaque, local particles	fair, slight agglomeration
M5	0.075	black and opaque, rough surface	poor, obvious agglomeration

3.1.2 Swelling Property

The swelling ratios of all hydrogel groups are summarized in Table 2. The pure chitosan hydrogel exhibited the highest swelling ratio but was susceptible to deformation post-swelling. With increasing MWCNT loading, the swelling ratio first rose and then decreased; Group M3 (0.045 g) achieved the maximum value of 1786% and retained intact morphology without deformation upon swelling.

The incorporation of moderate MWCNTs increases the porosity of the hydrogel network and enhances water uptake capacity, while hydrogen bonding between MWCNTs and chitosan chains reinforces network structural stability and prevents swelling-induced collapse. In contrast, excessive MWCNT loading (> 0.045 g) triggers nanotube agglomeration, which elevates crosslinking density, reduces pore volume, impedes water diffusion, and ultimately lowers the swelling ratio [7].

ISSN 2616-5880 Vol. 7, Issue 1: 80-88, DOI: 10.25236/AJMC.2026.070112

3.1.3 Mechanical Property

The tensile property test results (Table 2) showed that with the increase of MWCNTs dosage, the tensile strength of the gel first increased and then decreased. The tensile strength of 4 group reached 39.1 kPa, which was 37.2% higher than that of pure chitosan gel (P<0.05), and the elongation at break also increased slightly.As a rigid reinforcing phase, MWCNTs can effectively transfer stress and exert fiber reinforcement effect. Meanwhile, the oxygen-containing groups on their surface form hydrogen bonds with the amino and hydroxyl groups of chitosan, which enhances the interfacial bonding force and improves the mechanical strength and toughness of the gel [8]. At excessive dosage, the agglomeration of carbon nanotubes forms stress concentration points, which leads to the decline of mechanical properties instead.Combining appearance, swelling, and mechanical properties, the optimal addition amount of MWCNTs was determined to be 0.045 g.

Table 2 Swelling ratio and tensile properties of gels with different MWCNTs dosages

Group	MWCNTs dosage / g	Equilibrium swelling ratio / %	Tensile strength/ kPa	Elongation at break / %
CS	0	1624	28.5	112
M1	0.015	1682	32.7	118
M2	0.030	1674	35.2	121
M3	0.045	1786	39.1	125
M4	0.060	1528	36.8	108
M5	0.075	1424	34.2	96

3.2 Optimization of LPNS Saponins Dosage

The encapsulation efficiency and drug loading capacity under different drug dosages are shown in Table 3. With the increase of *Panax notoginseng* leaf saponins dosage, the encapsulation efficiency increased rapidly at first and then leveled off, while the drug loading capacity increased continuously. When the dosage was 0.07 g, the encapsulation efficiency reached 97.47% and the drug loading capacity was 3.34%. When the dosage was further increased to 0.09 g, the encapsulation efficiency only increased by 0.31 percentage points, and the amount of free drug increased significantly.

This is because the adsorption sites of chitosan and MWCNTs are limited. At low drug dosage, drug molecules can be fully encapsulated through hydrogen bonding and hydrophobic interaction. When the drug dosage exceeds the saturated loading capacity of the carrier, the excess drug cannot be fixed and remains free in the gel matrix, resulting in no significant increase in encapsulation efficiency and increased risk of initial burst release [9]. Therefore, 0.07 g was selected as the optimal dosage of LPNS.

Table 3 Encapsulation efficiency and drug loading capacity under different drug dosages

MWCNTs dosage / g	drug dosage / g	encapsulation efficiency / %	drug loading capacity / %
0.015	0.05	96.43	2.36
0.030	0.06	97.25	2.85
0.045	0.07	97.47	3.34
0.060	0.08	97.68	3.82
0.075	0.09	97.78	4.30

3.3 FT-IR Spectroscopy Analysis

FT-IR characterization was performed on chitosan, MWCNTs, *Panax notoginseng* leaf saponins, and the optimal ratio composite gel, and the results are shown in Figure 1.

Chitosan showed a broad O—H and N—H stretching vibration peak at 3430 cm^{-1}, an amide I band C=O stretching vibration peak at 1655 cm^{-1}, and a C—O stretching vibration peak at 1 080 cm^{-1}. MWCNTs had a hydroxyl characteristic peak at 3420 cm^{-1} and a C=C skeleton vibration peak at 1630 cm^{-1}. LPNS showed a broad hydroxyl peak at 3 400 cm^{-1} and a glycosidic bond characteristic peak at 1070 cm^{-1}.

In the spectrum of the composite gel, the hydroxyl/amino stretching vibration peaks at 3 200–3500

ISSN 2616-5880 Vol. 7, Issue 1: 80-88, DOI: 10.25236/AJMC.2026.070112

cm^{-1} had weakened intensity, broadened peak shape, and shifted to lower wavenumbers, indicating that a large number of intermolecular hydrogen bonds were formed among the hydroxyl/amino groups of chitosan, the oxygen-containing groups on MWCNTs surface, and the hydroxyl groups of LPNS [10]. The superposition and shift of amide peaks and carbon skeleton peaks at 1620–1640 cm^{-1} proved the existence of electrostatic interactions among components. The mutual coupling of glycosidic bond and carbon-oxygen bond peaks at 1000–1100 cm^{-1}, without obvious sharp single peaks, indicated good compatibility among components and no obvious phase separation. The FT-IR results confirmed that the multi-components formed a stable three-dimensional composite network structure through non-covalent interactions.

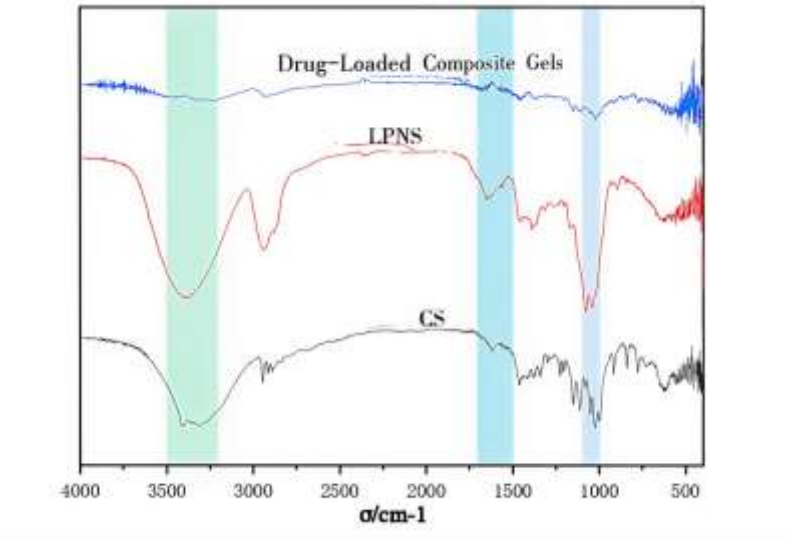

Figure 1 FT-IR characterization of CS LPNS and composite gel

3.4 Stability Evaluation of Composite Gel

3.4.1 Swelling Kinetics

The swelling kinetics of the optimal ratio composite gel in pH 7.4 PBS are shown in Table 4. The swelling process of the gel can be divided into two stages: rapid swelling and slow equilibrium. 0–2 h was the rapid swelling stage, where water molecules quickly entered the gel network, the polymer chains stretched, and the swelling ratio increased rapidly. The swelling rate gradually slowed down from 2 h to 4 h, and the swelling ratio reached 491% at 4 h, gradually approaching swelling equilibrium.

Compared with pure chitosan gel, the composite gel had a more gentle swelling rate and more stable morphology after equilibrium, indicating that the addition of MWCNTs enhanced the structural strength of the gel network, avoided structural collapse caused by rapid swelling, and was conducive to maintaining the stability of drug release.

Table 4 Swelling kinetics of the composite gel

Time / h	Dry gel mass / g	Mass after swelling / g	Swelling ratio / %
1	0.5	1.075	115
2	0.5	1.675	235
3	0.5	2.048	310
4	0.5	2.955	491

3.4.2 Cold and heat resistance

The cold and heat resistance test results are shown in Table 5. After being stored at 4 ℃ for 24 h, the composite gel had no cracking or shrinkage, with uniform texture and a mass retention rate of 97.5%, which was significantly better than that of pure chitosan gel (92.3%). After being stored at 60 ℃ for 24 h, the composite gel showed slight water loss and shrinkage with slightly increased hardness, but the overall morphology was intact without fragmentation, with a mass retention rate of 70.3%, while pure chitosan gel showed obvious softening and deformation.MWCNTs have excellent thermal conductivity and thermal stability. They can form heat conduction paths in the gel network to relieve local thermal stress. Meanwhile, the enhanced hydrogen bond network can improve the thermal stability of polymer

ISSN 2616-5880 Vol. 7, Issue 1: 80-88, DOI: 10.25236/AJMC.2026.070112

chains, thus improving the cold and heat resistance of the gel [11]. This result indicates that the composite gel can adapt to temperature fluctuations during conventional storage and transportation, with good environmental adaptability.

Table 5 Cold and heat resistance of the composite gel

Environmental condition	Treatment time / h	Initial mass / g	Mass after treatment / g	Mass retention rate / %	Appearance change
4 ℃	12	1.0	0.982	98.2	No obvious change
	24	1.0	0.975	97.5	Intact morphology, no cracking
60 ℃	12	1.0	0.816	81.6	Slight water loss and shrinkage
	24	1.0	0.703	70.3	Obvious water loss, slightly increased hardness, no fragmentation

3.5 In Vitro sustained-release performance and release mechanism

3.5.1 In Vitro release curves

The *in vitro* cumulative release curves of CS drug-loaded gel and composite drug-loaded gel are shown in Figure 2. The release processes of both groups showed the characteristics of "rapid initial release and slow release in the middle and late stages", but there were significant differences:

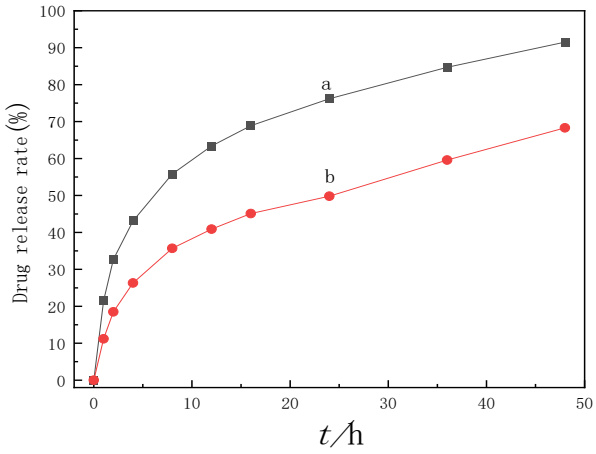

Figure 2. Drug release rate of CS drug-loaded gel(a) and composite drug-loaded gel(b)

Initial stage (0–2 h):CS gel showed obvious burst release, with a cumulative release rate of 32.7% at 2 h; the composite gel only had a cumulative release rate of 18.5% at 2 h, with a significantly reduced burst release amplitude. This is because the adsorption effect and network barrier effect of MWCNTs reduce the rapid diffusion of free drugs on the gel surface.

Sustained-release stage (2–24 h): Pure chitosan gel had a fast release rate, with a cumulative release rate of 76.2% at 24 h; the composite gel released steadily and slowly, with a cumulative release rate of 49.8% at 24 h.

Plateau stage (24–48 h): The cumulative release rate of pure chitosan gel reached 91.5% at 48 h, and the drug was almost completely released; the composite gel had a cumulative release rate of 68.3% at 48 h, still maintaining a continuous release trend.

The above results indicate that the introduction of MWCNTs can significantly delay the release of LPNS and enhance the sustained-release effect. The action mechanism mainly includes two aspects: first,

ISSN 2616-5880 Vol. 7, Issue 1: 80-88, DOI: 10.25236/AJMC.2026.070112

the large specific surface area of MWCNTs can adsorb drug molecules through hydrogen bonding and hydrophobic interaction, increase drug binding sites, and reduce the proportion of free drugs; second, MWCNTs filled in the three-dimensional chitosan network prolong the diffusion path of drug molecules and increase the mass transfer resistance, thus delaying drug release [12].

3.5.2 Release kinetics fitting

Four common kinetic models were used to fit the release data of the composite gel, and the fitting parameters are shown in Table 6.

Table 6 Fitting parameters of drug release kinetic models

Kinetic model	Fitting equation	Correlation coefficient R^2
Zero-order model	Q=1.3827t+12.564	0.9125
First-order model	ln(100-Q)=-0.0241t+4.5823	0.9687
Higuchi model	Q=8.7652$t^{1/2}$+2.1436	0.9912
Ritger-Peppas model	ln$Q$=0.4283ln$t$+2.3571	0.9846

As shown in Table 6, the Higuchi model had the highest correlation coefficient (R^2=0.9912), indicating that drug release was dominated by diffusion mechanism. The release index n of the Ritger-Peppas model was 0.4283 (n<0.45), which further confirmed that the release mechanism was Fickian diffusion, that is, the diffusion of drug molecules through the gel network pores was the main rate-limiting step of release [13]. This is consistent with the FT-IR analysis results: the dense hydrogen bond network formed among components and the barrier effect of MWCNTs jointly increase the drug diffusion resistance and achieve the sustained-release effect.

4. Conclusions

In this work, an LPNS-loaded MWCNT/chitosan composite hydrogel was successfully fabricated, with its formulation optimized via single-factor experiments and its microstructure and physicochemical properties systematically characterized. The main conclusions are drawn as follows:

The optimal formulation was identified as 0.045 g MWCNTs and 0.07 g LPNS. Under this condition, the composite hydrogel achieved homogeneous dispersion, with a 37.2% enhancement in tensile strength relative to pure chitosan hydrogel, an encapsulation efficiency of 97.47%, and a drug loading capacity of 3.34%.

FT-IR analysis confirmed that all components assembled into a stable three-dimensional network through hydrogen bonding and electrostatic interactions. The composite hydrogel exhibited moderate swelling behavior in pH 7.4 PBS and possessed markedly superior thermal stability compared with pure chitosan hydrogel.

In vitro release studies revealed that the composite hydrogel effectively attenuated the initial burst release, with a cumulative drug release of 68.3% at 48 h. The release kinetics fitted well to the Higuchi model and were governed by a Fickian diffusion mechanism, demonstrating excellent long-term sustained-release performance.

This study provides a promising carrier candidate for the local sustained delivery of Panax notoginseng leaf saponins. Future work should focus on cytocompatibility evaluation, in vivo pharmacodynamic studies, and MWCNT surface modification to facilitate the translational application of the composite hydrogel.

References

[1] Zhang Y, Liu M, Wang H, et al. Biodegradation and biocompatibility of chitosan-based hydrogels for biomedical applications [J]. International Journal of Biological Macromolecules, 2023, 242: 124897.
[2] Muxika A, Etxabide J, Uranga J, et al. Chitosan as a bioactive polymer: Processing, properties and applications for drug delivery [J]. International Journal of Biological Macromolecules, 2022, 213: 674-689.
[3] Liu X, Zhou J, Chen Z, et al. Reinforcement of chitosan hydrogels with functionalized multi-walled carbon nanotubes: mechanical and structural properties [J]. Journal of Materials Science: Materials in

ISSN 2616-5880 Vol. 7, Issue 1: 80-88, DOI: 10.25236/AJMC.2026.070112

Medicine, 2024, 35(2): 45.
[4] Liu Y, Chen L, Wang H, et al. MWCNT-reinforced chitosan composite hydrogels with enhanced mechanical strength and sustained drug release performance [J]. Carbohydrate Polymers, 2023, 316: 121056.
[5] Xi Y, Yang L, Wang Y, et al. Sodium alginate/chitosan hydrogels loaded with herbal active ingredients for promoting deep second-degree scald wound healing in rats [J]. Journal of Ethnopharmacology, 2023, 307: 116245.
[6] Zhang Z, Li M, Zhou X. Dispersion behavior of multi-walled carbon nanotubes in chitosan matrix: mechanism and influencing factors [J]. Colloids and Surfaces A: Physicochemical and Engineering Aspects, 2023, 667: 131398.
[7] Chen M, Zhao X, Li Y. Effect of nanofiller loading on swelling kinetics and network structure of chitosan composite hydrogels [J]. Journal of Applied Polymer Science, 2023, 140(24): e54127.
[8] Li Y, Sun H, Zhao J, et al. Mechanical enhancement of polymer hydrogels via carbon nanotube-reinforced photopolymerized network [J]. Polymer Testing, 2023, 124: 108075.
[9] Jiang K, Ding M, Ye T, et al. Sustained-release properties of β-chitosan hydrogel carriers for hydrophilic active ingredients [J]. International Journal of Pharmaceutics, 2022, 624: 121986.
[10] Zhao G, Yang J, Wang Y, et al. Interfacial interactions and electromechanical properties of chitosan/carbon nanotube composite hydrogel actuators [J]. Sensors and Actuators A: Physical, 2023, 356: 114362.
[11] Srivastava A, Mishra S. Thermal and mechanical stability of carbon nanotube-reinforced chitosan hydrogels [J]. Thermochimica Acta, 2022, 713: 179236.
[12] Nithya S, Nimal T, Baranwal G, et al. Sustained release and antibacterial efficacy of bioactive-loaded chitosan composite hydrogels [J]. International Journal of Biological Macromolecules, 2024, 263: 130215.
[13] Wang L, Wu X, Ma L, et al. Thermosensitive chitosan/sodium glycerophosphate hydrogels for sustained protein delivery: release kinetics and mechanism [J]. International Journal of Biological Macromolecules, 2022, 219: 847-856.